Competition in rotation-alignment between high-j neutrons and protons in transfermium nuclei

Falih Al-Khudair[1,2,3], Gui-Lu Long[1,2], Yang Sun[4,5]*
[1]*Department of Physics, Tsinghua University, Beijing 100084, People's Republic of China*
[2]*Center of Nuclear Theory, Lanzhou National Laboratory of Heavy Ion Accelerator, Lanzhou 730000, People's Republic of China*
[3]*Department of Physics, College of Education, Basrah University, Basrah, Iraq*
[4]*Department of Physics, Shanghai Jiao Tong University, Shanghai 200240, People's Republic of China*
[5]*Institute of Modern Physics, Chinese Academy of Sciences, Lanzhou 730000, People's Republic of China*
(Dated: March 4, 2009)

The study of rotation-alignment of quasiparticles probes sensitively the properties of high-j intruder orbits. The distribution of very high-j orbits, which are consequences of the fundamental spin-orbit interaction, links with the important question of single-particle levels in superheavy nuclei. With the deformed single-particle states generated by the standard Nilsson potential, we perform Projected-Shell-Model calculations for transfermium nuclei where detailed spectroscopy experiment is currently possible. Specifically, we study the systematical behavior of rotation-alignment and associated band-crossing phenomenon in Cf, Fm, and No isotopes. Neutrons and protons from the high-j orbits are found to compete strongly in rotation-alignment, which gives rise to testable effects. Observation of these effects will provide direct information on the single-particle states in the heaviest nuclear mass region.

PACS numbers: 21.10.Re, 21.60.Cs, 27.90.+b

I. INTRODUCTION

The occurrence of superheavy elements (SHE) is attributed to the nuclear shell effect because the macroscopic liquid-drop model would predict that such heavy elements can not exist due to large Coulomb repulsive force. The distribution of single-particle (SP) states as a consequence of the shell effect has thus become the discussion focus in the SHE problem. One important question has been where are the next magic numbers in the superheavy mass region beyond the known magic number 126 for neutrons and 82 for protons. The precise location of the new magic numbers depends sensitively on the SP structure. Theoretically, stability is predicted for the nuclei close to the spherical shells with $N = 184$ and $Z = 114$ (also $Z = 120$ or 126, depending on theoretical models employed), which suggests the existence of "island of stability" [1] next to the well-known doubly-magic nucleus ^{208}Pb.

Exploring the island is the current goal in nuclear science. In the past few years, researchers have made significant progress in synthesis of new elements (for review, see Refs. [2, 3, 4, 5]). Presently, little is known about their structure. The heaviest nuclei for which detailed spectroscopy measurement can be performed lie in the transfermium mass region, as for instance, the Californium, Fermium, and Nobelium isotopes [6, 7, 8, 9]. These nuclei, typically with $N \approx 100$ and $Z \approx 150-160$, are not really SHE. However, they are at the gateway to the SHE region, and furthermore, are well deformed. As one can clearly see form the deformed SP spectra [10] that with deformation, the Fermi surfaces of these nuclei are surrounded by some orbitals originating from the subshells near the anticipated new magic numbers. Thus, the study of these deformed transfermium nuclei may provide an indirect way to access the SP states of the closed spherical shells, which are of direct relevance to the location of the predicted island.

In-beam measurements for the transfermium region have been performed for yrast γ-ray spectroscopy of even-even nuclei (for example, ^{250}Fm [11], ^{252}No [12], ^{254}No [13]). The data reveal that these nuclei are well deformed. At low-spins near the ground state, they all exhibit very similar collective behavior with regular rotational level sequence. This tells us that near the ground state, these nuclei behave like a heavy, rigid rotor. They show a strong collectivity, diluting any individual role of single-particles. Therefore, not much information can be extracted from these low-spin rotor states.

More useful information may be obtained through the study of high-spin states with quasiparticle excitations. In fact, some non-yrast and isomeric states have been observed (see, for example, Refs. [14, 15, 16, 17, 18, 19, 20, 21], and for the most recent review, see Ref. [9]). The yielded data contain useful information on excited levels and configurations of multi-quasiparticle states in this mass region, and moreover, they test strictly current nuclear models that have been used for prediction. There are several types of quasiparticle excitation. One possibility is the study of K-isomers through the isomer spectroscopy measurement [22]. The isomer study has become an important branch of nuclear structure research [23]. The suggestion of Xu *et al.* [24] has made the study of isomeric states in SHE more interesting. These authors suggested that the occurrence of isomeric states in SHE can enhance the stability because the multi-quasiparticle excitations decrease the probability for both nuclear fission and α-decay. In the present paper, we concentrate on another possibility of quasiparticle excitations; namely, we discuss rotation-alignment at high spins along the yrast line.

On the theoretical side, the early study by Munitian *et al.* on rotational structure in very heavy nuclei employed cranking approximation based on a macroscopic-microscopic approach [25]. The first microscopic calculation in the framework of the Hartree-Fock-Bogoliubov (HFB) approximation

*corresponding author: sunyang@sjtu.edu.cn

was carried out by Egido and Robledo in Ref. [26], in which properties of the ground-state rotational band in ^{254}No were discussed in detail. Subsequent studies include the cranked HFB calculations with the Skyrme force [27, 28], cranked HFB calculations with the Gogny force [29], cranked relativistic Hartree-Bogoliubov method [30], and very recently, cranked shell model with particle-number-conserving treatment [31]. In all these papers, cranking approximation was adopted to describe rotation and discussions were carried out in the intrinsic frame. Alternatively, Hess and Misicu [32] used the pseudo-symplectic description for low-spin collective motions in superheavy nuclei.

The present work is based on the Projected Shell Model (PSM) [33], and aims at understanding the role of high-j intruder orbits in the high-spin states of transfermium nuclei. It has been shown that the PSM describes efficiently the high-spin phenomena such as band-crossing, rotation-alignment, and band-bending in moment of inertia in well deformed nuclei. The present study systematically covers the isotopic chains of Californium, Fermium, and Nobelium, for states up to angular momentum $30\hbar$, well beyond the first band-crossing. Our method is different from the cranking approximations in that the PSM works in the laboratory frame in terms of the configuration mixing, and the observables such as electromagnetic transition rates can be unambiguously computed in the PSM framework. The PSM is thus free from the well-known problem occurring at the band-crossing region caused by the cranking approximation [34]. This is important for a theoretical treatment on band-crossings because the current experiment on transfermium nuclei is approaching the high-spin regions across the first band-crossing.

The paper is organized as follows. In Sec. II, we outline the theoretical mehtod. Systematic analysis of the rotational structure along the yrast line for even-even transfermium nuclei is carried out in Sec. III. Discussions about the present results and their implications are given in Sec. IV. Finally, a summary is given in Sec. V.

II. OUTLINE OF THE PROJECTED SHELL MODEL

A successful description of deformed nuclei can be traced back to the introduction of the Nilsson model [35]. In the Nilsson model, nuclear states are described by considering nucleons moving in a deformed potential. Deformed states are defined in the body-fixed frame of reference in which the rotational symmetry is broken. Although physics may be discussed in such an intrinsic frame, the broken rotational symmetry should in principle be recovered giving the fact that angular momentum is probably the most important quantum number in nuclear physics. Restoration of rotational symmetry is the first step of going beyond mean field, which can be done by using the angular-momentum-projection method [36]. The next step follows closely the basic strategy of the conventional shell model: The projected states are then regarded as a new basis in which one builds many-body wave functions in the laboratory frame, and a two-body shell model Hamiltonian is diagonalized in the projected basis. This means that one can use the deformed Nilsson SP states as an effective basis. Thus, the difference between the conventional shell model and the approach with angular-momentum-projection is that one employs a spherical basis to construct shell model basis in the former and a (projected) deformed basis in the latter.

The above idea of performing shell model calculations is practiced by the Projected Shell Model [33], which has been proven successful in the description of heavy, deformed nuclei. The calculation procedure is as follows. The PSM first constructs its shell-model basis by using the deformed Nilsson SP states (with the Nilsson parameters given in Ref. [37]) at a quadrupole deformation ε_2. Pairing correlations are incorporated into the Nilsson states by a BCS calculation. The consequence of the Nilsson-BCS calculations defines a set of quasiparticle (qp) states associated with the qp vacuum $|\phi(\varepsilon_2)\rangle \equiv |0\rangle$. One then considers the following multi-qp configurations for even-even nuclei

$$|\Phi_\kappa\rangle = \left\{ |0\rangle,\ \alpha^\dagger_{n_i}\alpha^\dagger_{n_j}|0\rangle,\ \alpha^\dagger_{p_i}\alpha^\dagger_{p_j}|0\rangle,\ \alpha^\dagger_{n_i}\alpha^\dagger_{n_j}\alpha^\dagger_{p_i}\alpha^\dagger_{p_j}|0\rangle \right\}, \tag{1}$$

where $\alpha^\dagger$ is the qp creation operator and the index n (p) denotes neutron (proton) Nilsson quantum numbers in orbitals. The angular-momentum-projected multi-qp states serve as the building blocks of our shell model basis, and the trail wave functions can be written as a superposition of them:

$$|\Psi^I_M\rangle = \sum_\kappa f^I_\kappa \hat{P}^I_{MK_\kappa}|\Phi_\kappa\rangle, \tag{2}$$

where $\hat{P}^I_{MK}$ is the angular-momentum projection operator [36]

$$\hat{P}^I_{MK} = \frac{2I+1}{8\pi^2}\int d\Omega D^I_{MK}(\Omega)\hat{R}(\Omega), \tag{3}$$

and κ labels the basis states. It is the angular momentum projection [33] that transforms the wave functions from the intrinsic frame to the laboratory frame. Finally a two-body Hamiltonian is diagonalized in the projected states (2) and the diagonalization determines f^I_κ. For details of how to perform a projection calculation, we refer to the PSM review article [33].

We use the pairing plus quadrupole-quadrupole (QQ) Hamiltonian with inclusion of both the monopole- and quadrupole-pairing terms

$$\hat{H} = \hat{H}_0 - \frac{1}{2}\chi\sum_\mu \hat{Q}^\dagger_\mu\hat{Q}_\mu - G_M\hat{P}^\dagger\hat{P} - G_Q\sum_\mu \hat{P}^\dagger_\mu\hat{P}_\mu. \tag{4}$$

In Eq. (4), $\hat{H}_0$ is the spherical SP Hamiltonian. The QQ-force strength χ is determined in such a way that it holds a self-consistent relation [33] with the quadrupole deformation ε_2 (given in Table I below). The monopole-pairing strength G_M is of the form

$$G_M = \frac{21.24 \mp 13.86\frac{N-Z}{A}}{A}, \tag{5}$$

with "$-$" for neutrons and "$+$" for protons. The quadrupole-pairing strength G_Q is assumed to be proportional to G_M,

TABLE I: Input deformation parameters (ε_2) used in the calculation.

Nucleus	^{246}Cf	^{248}Cf	^{250}Cf	^{252}Cf	^{250}Fm	^{252}Fm	^{254}Fm	^{256}Fm	^{252}No	^{254}No	^{256}No	^{258}No
ε_2	0.255	0.260	0.265	0.245	0.240	0.255	0.250	0.222	0.224	0.260	0.250	0.230

with the proportionality constant 0.12. We note that G_Q is an adjustable parameter of the PSM [33], and the quadrupole-pairing force has an effect of shifting the position of rotation-alignment [38]. At present, no definite data can say about the rotation-alignment in this mass region, and there is no motivation for us to use G_Q's other than the present one that reasonably described known yrast states and γ-vabrational states [39]. As the valence SP space, we include three major shells, $N = 5,6,7$ (4,5,6), for neutrons (protons). The deformed Nilsson SP states are generated with deformation parameters ε_2 listed in Table I, which are either obtained from experimental data, if available, or from mean-field calculations. We note that deformation in nuclei is a model-dependent concept. Our deformations are input parameters for the deformed basis, and in principle, it is not required that the numbers in Table I are exactly the same as deformation parameters used in other models. Nevertheless, it turns out that our employed deformation parameters Ref. [39] for this mass region are very close to those calculated in Refs. [40, 41], and follow the same variation trend along an isotopic chain as predicted by other models (for example, the most deformed isotope has the neutron number 152 and a decreasing trend for heavier isotopes is expected).

Once the wave functions of Eq. (2) are obtained, one can use them to directly calculate electromagnetic transition probabilities [42]. The B(E2) value that measures the electric quadrupole transition rate from an initial state I to a final state $I-2$ is given by

$$B(E2, I \to I-2) = \frac{1}{2I+1} |\langle \Psi^{I-2} || \hat{Q}_2 || \Psi^I \rangle|^2, \qquad (6)$$

where wave functions $|\Psi^I\rangle$ are those in Eq. (2). The effective charges used in our calculation are the standard ones: $e^\pi = 1.5e$ and $e^\nu = 0.5e$, which are fixed for all nuclei studied in this paper. Thus any variations in calculated B(E2)'s are subject to the structure change in wave functions.

The gyromagnetic factor (g factor) is the quantity most sensitive to the SP components in wave functions as well as to their interplay with collective degrees of freedom. Because of the intrinsically opposite signs of the neutron and proton g_s, a study of g factors enables the determination of the microscopic structure for underlying states. For example, variation of g factors often is a clear indicator for a SP component that strongly influences the total wave function. In the PSM, g factors can be directly computed by

$$g(I) = \frac{\mu(I)}{\mu_N I} = \frac{1}{\mu_N I} [\mu_\pi(I) + \mu_\nu(I)], \qquad (7)$$

with $\mu_\tau(I)$ being the magnetic moment of a state $|\Psi^I\rangle$, expressed as

$$\begin{aligned} \mu_\tau(I) &= \langle \Psi^I_I | \hat{\mu}^\tau_z | \Psi^I_I \rangle \\ &= \frac{I}{\sqrt{I(I+1)}} \langle \Psi^I || \hat{\mu}^\tau || \Psi^I \rangle \\ &= \frac{I}{\sqrt{I(I+1)}} \left[g^\tau_l \langle \Psi^I || \hat{j}^\tau || \Psi^I \rangle + (g^\tau_s - g^\tau_l) \langle \Psi^I || \hat{s}^\tau || \Psi^I \rangle \right], \end{aligned}$$

where $\tau = \pi$ and ν for protons and neutrons, respectively. The following standard values for g_l and g_s appearing in the above quation are taken:

$$\begin{aligned} g^\pi_l &= 1, \quad g^\pi_s = 5.586 \times 0.75, \\ g^\nu_l &= 0, \quad g^\nu_s = -3.826 \times 0.75. \end{aligned}$$

g^π_s and g^ν_s are damped by a usual 0.75 factor from the free-nucleon values to account for the core-polarization and meson-exchange current corrections [43]. These same values are used for all g factor calculations in the present paper, as in the previous PSM calculations, without any adjustment.

III. ANALYSIS OF ROTATIONAL STRUCTURE ALONG THE YRAST LINE

The nucleon response to the collective rotation is generally understood as follows. Near the non-rotating ground state of a nucleus, like-nucleons are paired and interact coherently to form a superfluid system. When a nucleus is rotating, the Coriolis anti-pairing force acts on the pairs, and the force increases with rotation. At a certain critical angular momentum one would expect that the pairs are all broken, and a phase transition from the superfluid to the normal-state phase would be observed [44]. However, nucleons move in orbits. Nucleons in different orbitals feel the Coriolis force very differently. Detailed analysis has shown that the Coriolis force is proportional to the size of the SP angular momentum j of a nucleon under consideration. Nucleons in the vicinity of the Fermi surface usually occupy several orbitals with different j-values, and one expects those nucleons with the highest j-value to break first and align their rotation along the rotational axis [45]. This is the real situation happening in a rotating nuclear system, known as the Stephens-Simon effect. It suggests that near the yrast line, rotation-alignment of particular high-j particles rather than a collapse of entire pairing correlation is the dominant mode. These high-j orbitals are usually the intruder states that have an opposite parity to their neighboring ones. Rotation-alignment lowers the energy of the high-j configurations, and at a certain angular momentum, the states with aligning nucleons becomes so low energetically that the qp aligning bands can cross the ground state band (g-band), constituting a situation of so-called band-crossing.

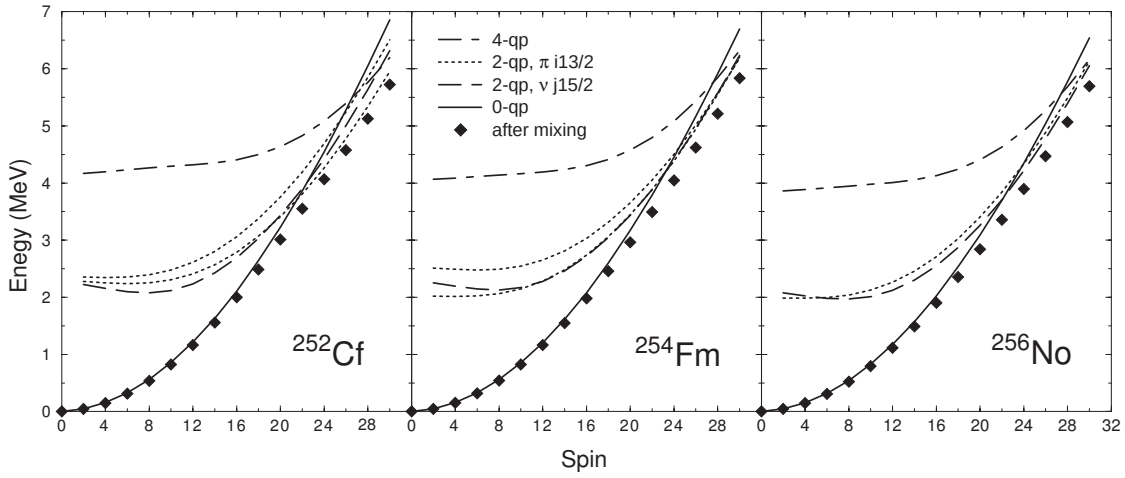

FIG. 1: Band diagrams for ^{252}Cf, ^{254}Fm, and ^{256}No. Several important configurations are shown: 0-qp (solid curves) starting from the origin, neutron 2-qp (dashed curves) and proton 2-qp (dotted curves) starting from 2 – 2.5 MeV, and 4-qp (dotted-dashed curves) starting from about 4 MeV. Filled diamonds denote the yrast states obtained after configuration mixing.

Rotation-alignment is a well-known phenomenon in nuclear high-spin physics, which is expected to occur also in rotating transfermium nuclei that the present work studies. The characteristic feature of rotation-alignment in transfermium nuclei is that the aligning pairs come mainly from the two high-j intruder orbitals: proton pairs from the $i_{13/2}$ orbital and neutron pairs from the $j_{15/2}$ orbital. As we shall discuss below, the presence of these two high-j orbitals near the Fermi level and their response to rotation can lead to an interesting competing picture at the band crossing region, which may lead to observations.

A. Band diagram

A band diagram is a useful tool introduced in Ref. [46] to analyze the numerical results of the PSM. Each angular-momentum-projected state in Eq. (2) represents a rotational band. The first one, $\hat{P}^I_{M0}|0\rangle$, represents the g-band in which all the particles are paired. The remaining states represent bands built upon multi-quasiparticle states. We define rotational energy of a band κ by

$$E_\kappa(I) = \frac{\langle\Phi_\kappa|\hat{H}\hat{P}^I_{KK}|\Phi_\kappa\rangle}{\langle\Phi_\kappa|\hat{P}^I_{KK}|\Phi_\kappa\rangle}. \qquad (8)$$

It represents the expectation value of the Hamiltonian with respect to a projected quasi-particle state κ. A diagram in which rotational energies of various bands are plotted against spin I is referred to as a *band diagram* which contains incredibly rich information. For example, one may observe several band-crossings at various spins in a diagram. The first crossing is usually a crossing between an aligning 2-qp band and the g-band, physically corresponding to the first rotation-alignment of a high-j pair of quasiparticles.

In the present study for the transfermium region, we have found interesting band-crossing pictures. To illustrate them, we take representative examples, and show band diagrams in Fig. 1 for the chain of $N = 154$ isotones: ^{252}Cf, ^{254}Fm, and ^{256}No. As the neutron number is unchanged in an isotonic chain but the proton Fermi level varies with the shell filling, the relative position of proton and neutron Fermi levels, and therefore the SP states in the vicinity of the Fermi levels, differ in the three. In Fig. 1, those curves starting from 2 – 2.5 MeV are the bands with 2-qp high-j configurations (dotted and dashed curves for 2-qp proton and 2-qp neutron configurations, respectively). At low-spins, the g-band (0-qp configuration) is low, and is the dominant component in the yrast wave function. However, it is seen that in all the three diagrams, several 2-qp bands cross the g-band around spin $I = 24$ and become energetically lower after the band-crossing. With a careful inspection, very delicate differences in the three cases can be found: After the band-crossing, the lowest band in ^{252}Cf is a 2-qp band of $i_{13/2}$ protons (dotted curve) and in ^{256}No a 2-qp band of $j_{15/2}$ neutrons (dashed curve), whereas in ^{254}Fm, the lowest dotted and the dashed curves are nearly degenerate after the band-crossing.

The above observation suggests a picture that at the band-crossing region, proton and neutron 2-qp high-j configurations compete strongly in the yrast states at the band-crossing region. After the band-crossing, the proton (neutron) configuration dominates the yrast structure in ^{252}Cf (^{256}No). In ^{254}Fm, the strongest competition between the proton and neutron configurations is predicted. Consequences of the competition and the delicate differences in the yrast wave functions can lead to observable effects, particularly in the spin-dependent g factor which is very sensitive to the SP content in wave functions. In the following three subsections, we present respectively the PSM results for the Cf, Fm, and No isotopes.

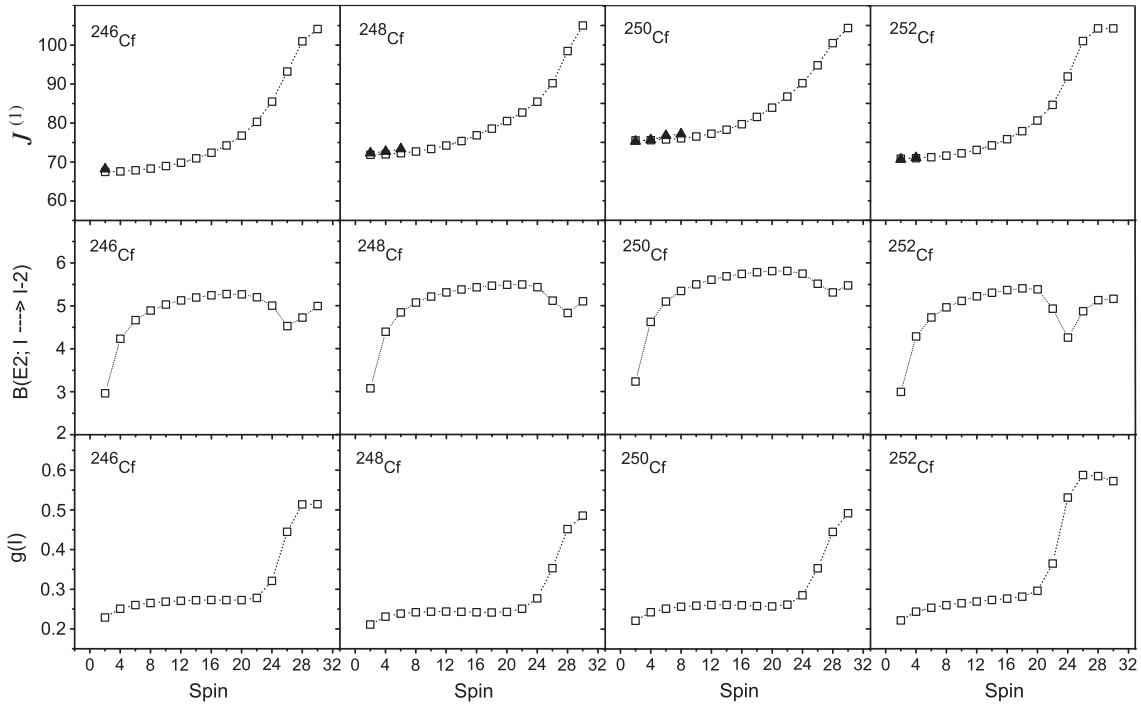

FIG. 2: Calculation for Californium isotopes. The top row of figures show the calculated static moments of inertia (open symbols), which are compared with available data (filled symbols). The middle and bottom row are the predicted B(E2) (in e^2b^2) and g factor values, respectively.

B. Cf isotopes

We present the calculated energy levels in terms of static moment of inertia defined by

$$\mathscr{J}^{(1)} = \frac{2I-1}{E(I)-E(I-2)}. \tag{9}$$

This quantity describes changes in band energies as spin varies. Experimental data on rotational spectrum in the transfermium region are still spare; we therefore compare our calculation with experiment whatever data are available, and make predictions where data do not exist. In addition, calculated $B(E2, I \to I-2)$ values defined in Eq. (6) and g factors in Eq. (7) are also presented.

Figure 2 shows the results for four Cf isotopes. In the top row, moments of inertia of these isotopes exhibit the following common behavior: At the low-spin region, they increase gently with spin, but climb more rapidly in the spin region between $I = 20$ to 30, showing a up-bending in moment of inertia. The spin region where the up-bending occurs corresponds to the place where bands cross to each other and rotation-alignment takes place, as discussed before. As shown in Fig. 2, only very limited experimental data points near the bandheads of each isotopes are known, with which our calculation agrees well.

The cause for the rapid rise in $\mathscr{J}^{(1)}$ in the high-spin region is attributed to rotation-alignment, which concerns the nature of the crossing band(s) with aligning pairs from high-j orbitals. It has already been seen in the energy-vs-spin plot (Fig. 1) that the rotationally-lowering of 2-qp bands leads to a crossing with the g-band. Among the lowest 2-qp bands that cross the g-band are those with 2-quasi-neutron configurations from the $j_{15/2}$ orbital and 2-quasi-proton ones from the $i_{13/2}$ orbital. These two kinds of configurations align their spins with very competitive probabilities. We find that for the Cf isotopes at deformation of $\varepsilon_2 \sim 0.24$, rotation-alignment of the $i_{13/2}$ 2-quasi-proton $K = 1$ state (coupled by $K = 5/2$ and $7/2$ $i_{13/2}$ quasi-protons) is the dominant configuration and is responsible for the rapid rise in moment of inertia in the Cf isotopes. This is a theoretical interpretation, and we need further experimental observations to support the picture.

Crossing of two bands with different configurations (here one fully-paired configuration and one configuration with high-j particle alignment) can cause a structure change for spin states before and after the crossing, which can lead to observable effects. Electromagnetic transition probability reflects such changes in wave functions. In the middle and bottom rows in Fig. 2, we present calculated B(E2) and g factor values, respectively. We observe that in all the isotopes, the B(E2) values increase smoothly with spin (The rapid rise near the band heads is due to the geometric Clebsch-Gordan coefficients), but with a drop around $I = 26$. The drop corresponds to smaller B(E2) values which are attributed to different structure in wave functions of the initial and the final state. In the g factor calculation, we observe a nearly-constant behavior for the low-spin states in all the four isotopes, but a sudden increase in the high spin region where rotation-alignment occurs. The rise is large, which nearly doubles the low-spin value of g factor. As only individual protons can bring positive contribution to the g factor and thus can accomplish the effect,

these results must imply a sudden increase in the proton component in the wave function. Detailed analysis shows that for the high-spin states with large g factors, the wave functions indeed have an increased amount of component from the proton $i_{13/2}$ orbit. Experiment of g factor at high-spins will be a strict test for our prediction, and in turn for the Nilsson SP states employed in our model.

C. Fm isotopes

In Fig. 3, we show the results for four Fm isotopes. The moments of inertia in the top row exhibit a similar behavior as in the Cf isotopes. As can be seen, our calculation reproduces the known data well. In particular, the yrast band in ^{250}Fm [11] was measured up to $I = 18$, for which the PSM calculation yields an excellent description. Comparing these four isotopes, the calculation predicts a more rapid rise in $\mathcal{J}^{(1)}$ at high-spins in the heavier isotope ^{256}Fm.

It is interesting that for Fm isotopes, the lowest 2-qp bands that cross the g-band correspond to the states with $K = 1$ 2-quasi-neutrons from the $j_{15/2}$ orbital (coupled by the $K = 7/2$ and $9/2$ states) and $K = 1$ 2-quasi-protons from the $i_{13/2}$ orbital (coupled by the $K = 7/2$ and $9/2$ states), with very competitive probability. Therefore, a pair of $j_{15/2}$ neutrons and a pair of $i_{13/2}$ protons both contribute to rotation-alignment, which is the cause for the irregularity in moment of inertia in the Fm isotopes. Similar conclusion was also obtained by the cranked relativistic mean field calculation in Ref. [11]. Only in ^{256}Fm, rotation-alignment of a pair of $i_{13/2}$ protons is predicted by the current calculation to be more favored over neutrons.

In the middle row of Fig. 3, a smooth behavior in B(E2) values is obtained up to the highest spin state in the two lighter Fm isotopes, while a drop is predicted for high spin states in the two heavier ones. As for g factors presented in the bottom row, a common behavior is seen for all four isotopes for spin states before the band crossing, namely, the g factor values are nearly constant with only slight variations as a function of spin. The smooth variation continues at high spin states for ^{250,252,254}Fm, but for ^{256}Fm, a sudden rise is predicted. The situation for ^{256}Fm is thus very similar to the Cf isotopes discussed before: The increase in g factor at high spins is contributed by the aligning protons. Indeed, detailed analysis shows that the aligning particles are the protons from the $i_{13/2}$ orbital coupled by the $K = 7/2$ and 9/2 states, which increases the proton component in wave functions. On the other hand, the near-constant g factors at high spin states for ^{250,252,254}Fm are understood as a combined effect of proton- and neutron-alignment. The negative contribution from neutrons to the g factor is compensated by the positive contribution from protons, leaving the total g factor almost unchanged for the entire spin region.

D. No isotopes

We consider four No isotopes $^{252-258}$No. Yrast bands of the two lighter No isotopes ^{252,254}No were measured up to considerably high spins [12, 13]. These two nuclei are also the most theoretically studied examples. Egido and Robledo [26] found in their cranked Hartree-Fock-Bogoliubov calculation with the Gogny force that the first upbending in moment of inertia in ^{254}No is attributed to alignment of a pair of $i_{13/2}$ protons. The cranked relativistic Hartree-Bogoliubov calculation [30] suggested that a simultaneous alignment of the $i_{13/2}$ proton and $j_{15/2}$ neutron pairs is responsible for the changes in moments of inertia in both ^{252,254}No.

Fig. 4 shows the PSM results for four No isotopes. In the top row of Fig. 4, a comparison with the known ^{252,254}No data in terms of static moments of inertia $\mathcal{J}^{(1)}$ yields a good agreement. Beyond the existing data points, a continued steady increase in $\mathcal{J}^{(1)}$ is predicted by the present calculation for high spin states, which does not seemingly indicate an anomaly in moment of inertia caused by band-crossing. A more sensitive plot for dynamic moments of inertia $\mathcal{J}^{(2)}$ for these tow isotopes is shown in Fig. 5, in which the calculation suggests a down-turning in slope of $\mathcal{J}^{(2)}$ at $I = 24$ for ^{254}No. In ^{252}No, the calculated $\mathcal{J}^{(2)}$ shows a down-turning at $I = 22$, followed by a up-turning at $I = 26$. The current data points for both nuclei stop just before the turning points. Extension of experimental measurement to higher spins will test our prediction.

In the middle row of Fig. 4, the calculation predicts a smooth trend in B(E2) for the two lighter isotopes ^{252,254}No. Similar B(E2) behavior is obtained for their isotones ^{250,252}Fm (see Fig. 3). For the two heavier isotopes ^{256,258}No, a sharp drop in B(E2) is predicted at $I = 26$. Drop in B(E2) corresponds to a structure change in the yrast band caused by rotation-alignment; however the B(E2) values alone cannot distinguish whether the cause is due to protons or neutrons. In the bottom row of Fig. 4, we observe the following evolution in g factor as neutron number varies. In ^{252}No, we predict an increase in g factor starting from $I = 22$. As discussed before, the $i_{13/2}$ proton alignment is responsible for this behavior. In the next isotope ^{254}No, rather constant g factor is predicted, which is understood as in the case of ^{250,252,254}Fm where a canceling in the proton- and neutron-contribution to the g factor is expected. Moving to the heavier No isotopes, we predict a big drop in g factor at about $I = 24$. The reason for the decrease in g factor is due to a large component of the 2-quasi-neutron $K = 1$ state (coupled by the $K = 7/2$ and $9/2$ $j_{15/2}$ states) in the wave functions at and after the band-crossing. This suggests that for ^{256,258}No, the $j_{15/2}$ neutrons win in the proton-neutron alignment competition, and the high-j neutron component is dominant in the yrast wave functions at high spin states.

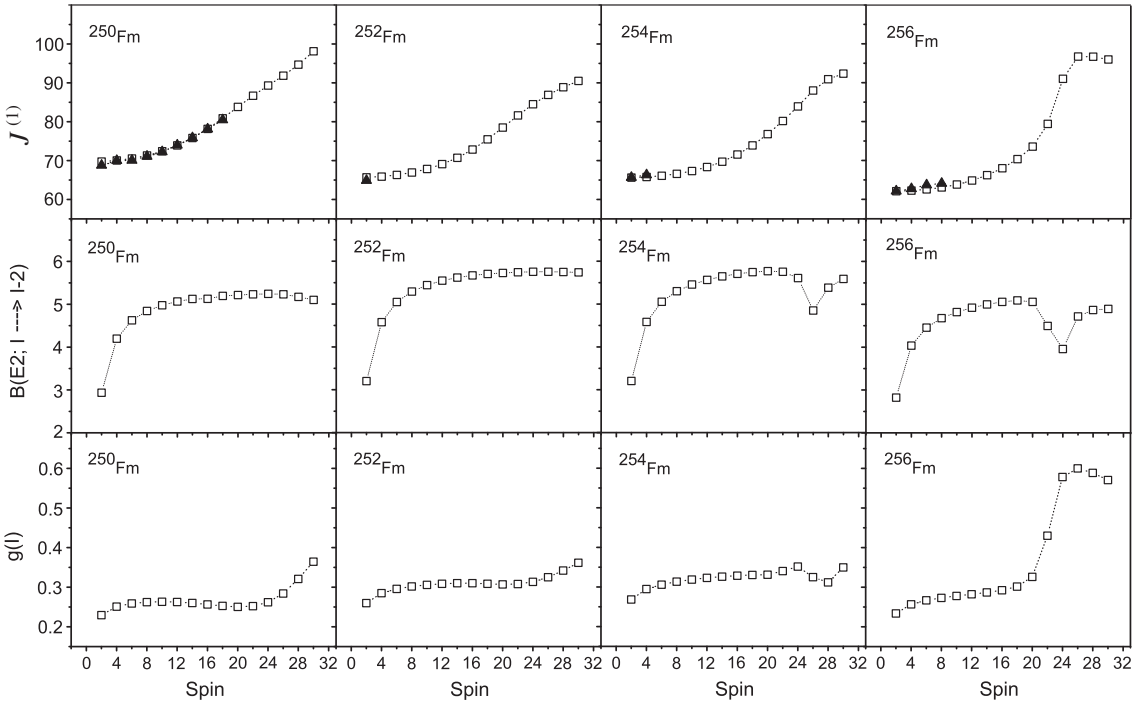

FIG. 3: Same as Fig.2, but for Fermium isotopes.

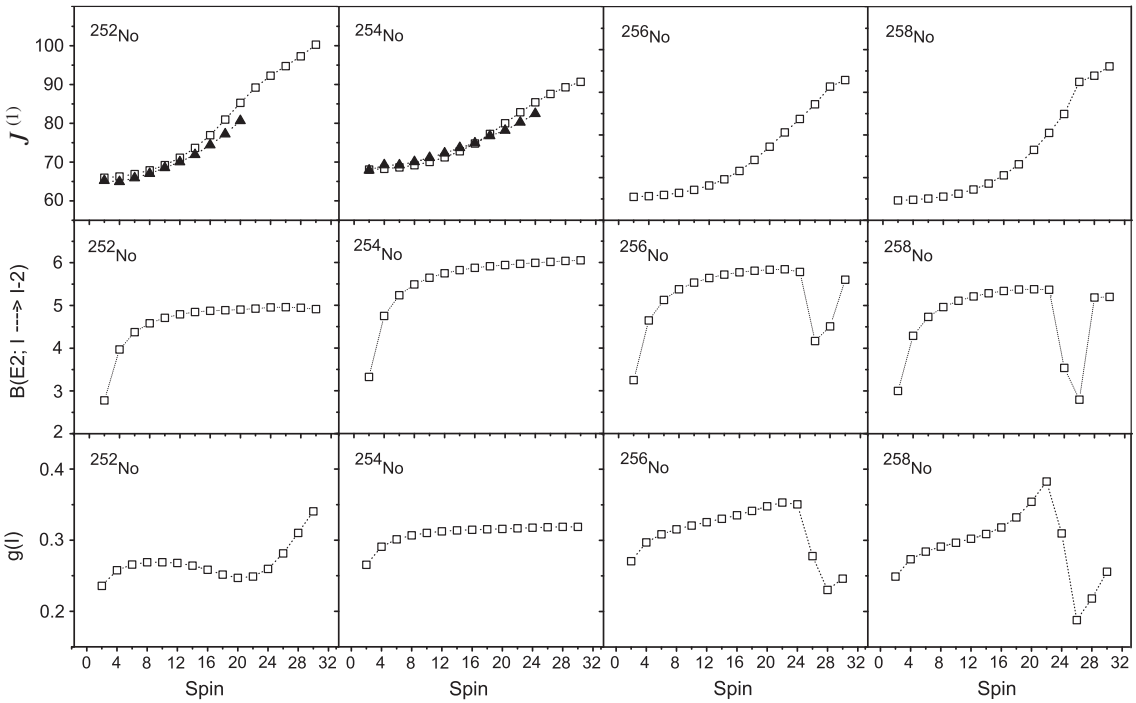

FIG. 4: Same as Fig. 2, but for Nobelium isotopes.

IV. DISCUSSIONS

The early work of Egido and Ring [47] studied the actinides nuclei using the rotating shell model with particle number projection and inclusion of quadrupole-pairing interaction. For the heaviest isotopes they studied, they obtained similar predictions for ^{244,246}Cf (in particular for g factors) as ours. They reached the same conclusion that there is a competition between proton and neutron alignment. For the alignment low K levels in the high j orbits are important. Filling in more and more particles one therefore has to provide more and more en-

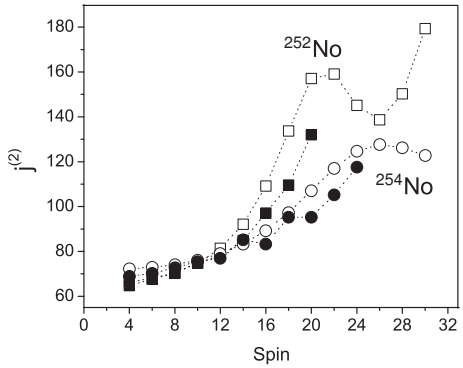

FIG. 5: Comparison of calculated dynamic moments of inertia $\mathcal{J}^{(2)}$ (open symbols) with experimental ones (filled symbols) for ^{252,254}No. $\mathcal{J}^{(2)}(I)$ is defined as $4/\Delta E_\gamma(I)$, with $\Delta E_\gamma(I) = E_\gamma(I) - E_\gamma(I-2) = E(I) - 2E(I-2) - E(I-4)$.

ergy in order to get alignment. In this mass region the neutron $j_{15/2}$ orbital contains generally more particles than the proton $i_{13/2}$ orbital. Therefore the alignment of protons is generally favored as compared to alignment of neutrons. That is what we have observed in all the four Cf isotopes as well as in ^{256}Fm and ^{252}No. Since nuclei are complex many-body systems, situation near the Fermi levels can change with neutron and proton numbers and a reversed case may occur. Moving away from heavier elements than what were discussed by Egido and Ring [47], we have found examples in which neutron alignment is more favored. In the heavier No isotopes, the present calculation suggests such examples.

However, from the energy levels alone we cannot easily distinguish proton and neutron contributions and a gradual, smooth alignment can hardly disentangled from the variable moment of inertia in the reference. B(E2) values cannot distinguish proton and neutron contributions either because one cannot experimentally separate the proton and neutron contributions to B(E2). A better probe in this regard is the magnetic moments through the study of g factors. g factors show rather clearly which kind of particle is aligning even in cases where no clear changes can be seen in the sequence of energy levels and in B(E2).

Our results presented in Figs. 2, 3, and 4, in particular those of g factor calculation, suggest a competition picture in rotation-alignment between the high-j intruder neutrons and protons. The delicate changes in wave functions result in distinct observables which can be tested in future experiment. These changes reflect nature of the rotation-aligning configurations and the characters of SP states for the transfermium region.

We have thus found measurable quantities that are sensitive to SP states, and therefore can serve as a testing ground. It is important to comment on the Nilsson SP states in the present calculation. Strictly speaking, SP states in deformed nuclei are not directly measurable. They are produced by calculations, and are model-dependent. Single-particle states in our shell-model basis are constructed by using the deformed Nilsson potential. Therefore, the above results and discussions depend on the Nilsson SP states. The adopted Nilsson parameters are the 1985 parameterisation of Bengtsson and Ragnarsson [37]. For the mass region of the present interest, this parameterisation gives a SP distribution very similar to another popular set of SP states produced by the Woods-Saxon potential of Chasman *et al.* [10]; the latter was used to assign configurations of the observed level structure in odd-mass transfermium nuclei [48, 49]. Thus in a sense, experimental confirmation or repudiation of the present PSM results is a test of the standard Nilsson model for the transfermium mass region.

V. SUMMARY

One of the key ingredients for locating the superheavy "island of stability" is the description of SP states. To predict SP states for SHE, extrapolation from existing microscopical models for the stable mass region is often assumed. However, the so-obtained SP states need to be carefully checked with experiment. Low-spin ground-state band in such heavy, deformed systems exhibits nothing but a collective rotor behavior, thus telling little useful information on SP states. To extract useful information from observables, one needs to study those excited configurations that directly carry information on individual particles. The present work attempts to understand the SP structure through the study of measurable quantities related to 2-qp excitations with rotation-alignment. The study has used the Projected Shell Model, which adopted the widely-used deformed Nilsson SP states as a starting basis, systematically performed shell model calculations for some Cf, Fm, and No isotopes, and compared the results with existing data in terms of moment of inertia. The calculation has further predicted B(E2) and g factor values for these nuclei.

Results of the present calculation can be summarized as follows. The static moments of inertia of all isotopes studied in this paper has been shown to have a similar behavior: At low-spin region, they increase gently with rotation, but a more rapid rise is seen in the spin region $I = 20$ to 30. The rise of $\mathcal{J}^{(1)}$ indicates additional contribution of angular momentum from the aligning quasiparticles. By studying band diagrams, we have found that the relevant quasiparticles are those from the high-j intruder orbitals with $i_{13/2}$ for protons and $j_{15/2}$ for neutrons. For all the three nuclei (^{250}Fm, ^{252}No, and ^{254}No) for which there exist longer sequence of experimental levels, our calculation has obtained a good agreement with data. We have found that the experimental states were measured just before the band-crossing spin. The prediction for the higher spin states awaits future experimental confirmation.

Electromagnetic transition properties reflect microscopic inside of wave functions, and thus are more sensitive probes for the structure. Study of energy levels alone cannot fully understand the microscopic origin of the rotation-alignment, and the variation in moment of inertia and B(E2). By studying g factors, we have found important differences in aligning particles. The proton-$i_{13/2}$ alignment is preferred for the Cf isotopes, as well as for ^{256}Fm. The strongest competition in rotation-alignment between the high-j protons and neutrons

has been suggested for the lighter Fm and No isotopes, in which g factors are predicted to stay nearly constant in the spin region where rotation-alignment takes place. Finally, the neutron-$j_{15/2}$ rotation-alignment is favored in the heavier No isotopes. It is expected that the future experiment, in particular g factor measurements, will provide a strict test for the current theory, and for the applicability of the standard Nilsson scheme [37] (also of the Woods-Saxon model [10] as its results are very similar to those of the Nilsson model) to the superheavy mass region.

Y.S. thanks the colleagues at Institute of Modern Physics, Tsinghua University, and Peking University, China, for the warm hospitality extended to him. This work was supported in part by the National Natural Science Foundation of China under contract No. 10325521 and 10875077, and by the Chinese Major State Basic Research Development Program through grant 2007CB815005.

[1] M. A. Stoyer, Nature **442**, 876 (2006).
[2] S. Hofmann and G. Münzenberg, Rev. Mod. Phys. **72**, 733 (2000).
[3] P. Armbruster, Annu. Rev. Nucl. Part. Sci **50**, 411 (2000).
[4] S. Hofmann, Prog. Part. Nucl. Phys. **46**, 293 (2001).
[5] Yu. Ts. Oganessian, Nucl. Phys. **A 787**, 343c (2007).
[6] M. Leino and F. P. Heßberger, Annu. Rev. Nucl. Part. Sci. **54** 175 (2004).
[7] R.-D. Herzberg, J. Phys. G **30**, R123 (2004).
[8] P. T. Greenlees, Nucl. Phys. **A 787**, 507c (2007).
[9] R.-D. Herzberg and P. T. Greenlees, Prog. Part. Nucl. Phys. **61**, 674 (2008).
[10] R. R. Chasman, I. Ahmad, A. M. Friedman, and J. R. Erskine, Rev. Mod. Phys. **49**, 833 (1977).
[11] J. E. Bastin *et al.*, Phys. Rev. C **73**, 024308 (2006).
[12] R.-D. Herzberg *et al.*, Phys. Rev. C **65**, 014303 (2001).
[13] P. Reiter *et al.*, Phys. Rev. Lett. **82**, 509 (1999).
[14] S. Hofmann *et al.*, Eur. Phys. J. A **10**, 5 (2001).
[15] P. A. Butler *et al.*, Phys. Rev. Lett. **89**, 202501 (2002).
[16] S. Eeckhaudt *et al.*, Eur. Phys. J. A **26**, 227 (2005).
[17] R.-D. Herzberg *et al.*, Nature **442**, 896 (2006).
[18] S. K. Tandel *et al.*, Phys. Rev. Lett. **97**, 082502 (2006).
[19] B. Sulignano *et al.*, Eur. Phys. J. A **33**, 327 (2007).
[20] K. Katori, I. Ahmad, and A. M. Friedman, Phys. Rev. C **78**, 014301 (2008).
[21] P. T. Greenlees *et al.*, Phys. Rev. C **78**, 021303(R) (2008).
[22] G. D. Jones, Nucl. Instrum. Meth. A **488**, 471 (2002).
[23] A. Aprahamian and Y. Sun, Nature Phys. 1, 81 (2005).
[24] F.-R. Xu, E.-G. Zhao, R. Wyss, and P. M. Walker, Phys. Rev. Lett. **92**, 252501 (2004).
[25] I. Muntian, Z. Patyk, and A. Sobiczewski, Phys. Rev. C **60**, 041302 (1999).
[26] J. L. Egido and L. M. Robledo, Phys. Rev. Lett. **85**, 1198 (2000).
[27] T. Duguet, P. Bonche, P.-H. Heenen, Nucl. Phys. **A 679**, 427 (2001).
[28] M. Bender, P. Bonche, T. Duguet, and P.-H. Heenen. Nucl. Phys. **A 723**, 354 (2003).
[29] J.-P. Delaroche, M. Girod, H. Goutte, J. Libert, Nucl. Phys. **A 771**, 103 (2006).
[30] A. V. Afanasjev, T. L. Khoo, S. Frauendorf, G. A. Lalazissis, and I. Ahmad, Phys. Rev. C **67**, 024309 (2003).
[31] X.-T. He, Z.-Z. Ren, S.-X. Liu, and E.-G. Zhao, Nucl. Phys. A, in press.
[32] P. O. Hess and S. Misicu, Phys. Rev. C **68**, 064303 (2003).
[33] K. Hara and Y. Sun, Int. J. Mod. Phys. E **4**, 637 (1995).
[34] I. Hamamoto, Nucl. Phys. **A 271**, 15 (1976).
[35] S. G. Nilsson, Mat. Fys. Medd. Dan. Vid. Selsk. **29**, No. 16 (1955).
[36] P. Ring and P. Schuck, *The Nuclear Many-Body Problem* (Springer-Verlag, New York, 1980).
[37] T. Bengtsson and I. Ragnarsson, Nucl. Phys. **A 436**, 14 (1985).
[38] Y. Sun, S.-X. Wen, D.-H. Feng, Phys. Rev. Lett. **72**, 3483 (1994).
[39] Y. Sun, F. Al-Khudair, G.-L. Long, and J. A. Sheikh, Phys. Rev. C **77**, 044307 (2008).
[40] S. Ćwiok, S. Hofmann, and W. Nazarewicz, Nucl. Phys. **A 573**, 356 (1994).
[41] P. Möller, J. R. Nix, W. D. Myers, and W. J. Swiatecki, At. Data Nucl. Data Tables **59**, 185 (1995).
[42] Y. Sun and J. L. Egido, Nucl. Phys. **A 580**, 1 (1994).
[43] B. Castel and I. S. Towner, *Modern Theories of Nuclear Moments* (Clarendon, Oxford, 1990).
[44] B. R. Mottelson and J. G. Valatin, Phys. Rev. Lett. **5**, 511 (1960).
[45] F. S. Stephens and R. S. Simon, Nucl. Phys. **A 183** (1972) 257.
[46] K. Hara and Y. Sun, Nucl. Phys. **A 529**, 445 (1991).
[47] J. L. Egido and P. Ring, Nucl. Phys. A **423**, 93 (1984).
[48] I. Ahmad *et al.*, Phys. Rev. C **72**, 054308 (2005).
[49] I. Ahmad *et al.*, Phys. Rev. C **71**, 054305 (2005).